

Few-shot Classification with Hypersphere Modeling of Prototypes

Ning Ding^{*1}, Yulin Chen^{*1}, Ganqu Cui¹, Xiaobin Wang²

Hai-Tao Zheng¹, Zhiyuan Liu¹, Pengjun Xie²

¹Tsinghua University, ²Alibaba Group

{dingn18, yl-chen21}@mails.tsinghua.edu.cn

Abstract

Metric-based meta-learning is one of the de facto standards in few-shot learning. It composes of representation learning and metrics calculation designs. Previous works construct class representations in different ways, varying from mean output embedding to covariance and distributions. However, using embeddings in space lacks expressivity and cannot capture class information robustly, while statistical complex modeling poses difficulty to metric designs. In this work, we use tensor fields (“areas”) to model classes from the geometrical perspective for few-shot learning. We present a simple and effective method, dubbed as hypersphere prototypes (HyperProto), where class information is represented by hyperspheres with dynamic sizes with two sets of learnable parameters: the hypersphere’s center and the radius. Extending from points to areas, hyperspheres are much more expressive than embeddings. Moreover, it is more convenient to perform metric-based classification with hypersphere prototypes than statistical modeling, as we only need to calculate the distance from a data point to the surface of the hypersphere. Following this idea, we also develop two variants of prototypes under other measurements. Extensive experiments and analysis on few-shot learning tasks across NLP and CV and comparison with 20+ competitive baselines demonstrate the effectiveness of our approach.

1 Introduction

Learning from a few examples, i.e., few-shot learning, is receiving increasing amounts of attention in modern deep learning. Because constituting cognition of novel concepts with few instances is crucial for machines to imitate human intelligence, and meanwhile, annotating large-scale supervised datasets is expensive and time-consuming (Lu et al., 2020). Although traditional deep neural

models have achieved tremendous success under sufficient supervision, it is still challenging to produce comparable performance when training examples are limited. Hence, a series of studies are proposed to generalize deep neural networks to low-data scenarios. One crucial branch of them is metric-based meta-learning (Reed, 1972; Nosofsky, 1986; Snell et al., 2017), where models are trained to generate expressive representations and carry out classification via defined metrics.

The success of metric-based learning depends on both *representation* learning and the *metrics* chosen. One straightforward approach relies on training feature representation and adopts a nearest-neighbor classifier (Vinyals et al., 2016; Yang and Katiyar, 2020; Wang et al., 2019). Other works introduce additional parameters as class representation to achieve better generalization ability. A naive way to estimate class representation is to use the mean embedding of feature representation (Snell et al., 2017; Allen et al., 2019), while some also use second-order moments (Li et al., 2019a) or reparameterize the learning process to generate class representation in a richer semantic space (Ravichandran et al., 2019) or in the form of probability distribution (Zhang et al., 2019). Apart from traditional Euclidean and cosine distance, a variety of metric functions are also proposed (Sung et al., 2018; Zhang et al., 2020a; Xie et al., 2022). Most existing works learn class representation from the statistical perspective, making designing and implementing the metrics more difficult. For example, the proposed covariance metric in CovaMNet (Li et al., 2019a) theoretically requires a non-singular covariance matrix, which is awkward for neural-based feature extraction methods.

This paper revisits metric-based learning and finds that geometrical modeling can simultaneously enhance the expressive ability of representations and reduce the difficulty of calculation, meanwhile yielding surprisingly effective performance in

^{*}Equal contribution

few-shot learning. Specifically, we propose `HyperProto`, a simple and effective approach to model class representation with hyperspheres. It is equipped with two advantages: the modeling is straightforward, and the corresponding metrics are easier to define and calculate compared to statistical methods. (1) For one thing, even if we attempt to use geometrical “areas” instead of “points” to represent class-level information, it is still difficult to explicitly characterize manifolds with complex boundaries in deep learning. But via hyperspheres modeling, we can obtain a hypersphere prototype with only two sets of parameters: the center and the radius of hyperspheres. (2) Besides, hyperspheres are suitable for constructing measurements in Euclidean space. We can calculate the Euclidean distance from one feature point to the surface of the hypersphere in order to perform metric-based classification, which is difficult for other manifolds.

We set the radii of the hyperspheres as learnable parameters, which makes it easy to combine the two advantages in few-shot learning. The distance from one feature point to the surface of a hypersphere prototype can be formalized as the distance from the point to the center of the hypersphere minus the radius. Thus, both the radius and the center of the hypersphere can appear in the loss function and participate in the backward propagation during optimization. Intuitively, for the classes with sparse feature distributions, the corresponding radii of their prototypes are large, and the radii are small otherwise. Beyond the Euclidean space, we also develop two variants based on the general idea – cone-like prototypes with cosine similarities and Gaussian prototypes from the probability perspective.

We conduct extensive experiments to evaluate the effectiveness of `HyperProto`. In addition to two classical tasks, few-shot named entity recognition (NER) (Ding et al., 2021c) and relation extraction (RE) (Han et al., 2018; Gao et al., 2019b) in NLP, we also assess our approach on few-shot image classification (Vinyals et al., 2016; Welinder et al., 2010), proving that it is a general method that could be applied to diverse scenarios. Despite the simplicity, we find that our approach is exceedingly effective, which outperforms the vanilla prototypes by 8.33 % absolute in average F1 on FEW-NERD (INTRA), 6.55% absolute in average F1 on FEW-NERD (INTER), 4.77% absolute in average accuracy on FewRel, 21.63% absolute in average accuracy on FewRel 2.0, and 3.45% absolute in

average accuracy on *miniImageNet*, respectively. Our method also yields better performance with 20+ competitive approaches across three tasks. Surprisingly, `HyperProto` performs more than satisfactorily in cross-domain few-shot relation extraction and cross-dataset image classification, indicating the promising ability in domain adaptation. Given that such small changes can bring considerable benefits, we believe our approach could serve as a strong baseline for few-shot learning and inspire new ideas from the research community for representation learning.

2 Problem Setup

We consider the episodic N -way K -shot few-shot classification paradigm¹. Given a large-scale annotated training set $\mathcal{D}_{\text{train}}$, our goal is to learn a model that can make accurate predictions for a set of new classes $\mathcal{D}_{\text{test}}$, containing only a few labeled examples for training. The model will be trained on episodes constructed using $\mathcal{D}_{\text{train}}$ and tested on episodes based on $\mathcal{D}_{\text{test}}$. Each episode contains a *support* set $\mathcal{S} = \{\mathbf{x}_i, y_i\}_{i=1}^{N \times K}$ for learning, with N classes and K examples for each class, and a *query* set for inference $\mathcal{Q} = \{\mathbf{x}_j^*, y_j^*\}_{j=1}^{N \times K'}$ of examples in the same N classes. Each input data is a vector $\mathbf{x}_i \in \mathbb{R}^L$ with the dimension of L and y_i is an index of the class label. For each input \mathbf{x}_i , let $f_\phi(\mathbf{x}_i) \in \mathbb{R}^D$ denote the D -dimensional output embedding of a neural network $f_\phi : \mathbb{R}^L \rightarrow \mathbb{R}^D$ parameterized by ϕ .

3 Methodology

This section introduces the mechanisms of hypersphere modeling of prototypes. One hypersphere prototype is represented by two parameters: the center and the radius of the hypersphere, which is first initialized via estimation and then optimized by gradient descent along with the encoder parameters.

3.1 Overview

We now introduce `HyperProto`, which are a set of hyperspheres in the embedding space D to abstractly represent the intrinsic features of classes. Formally, one prototype is defined by

$$\mathcal{B}^d(f_\phi, \mathbf{z}, \epsilon) := \{f_\phi(\mathbf{x}) \in \mathbb{R}^D : d(f_\phi(\mathbf{x}), \mathbf{z}) \leq \epsilon\}, \quad (1)$$

¹For the few-shot named entity recognition task (sequence labeling), the sampling strategy is slightly different (details in Appendix D).

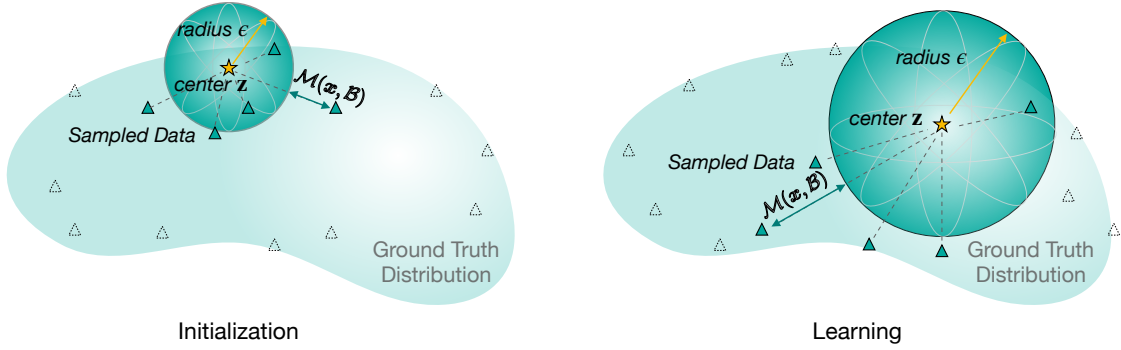


Figure 1: The illustration of our proposed *HyperProto*, where the data is sampled in 5-shot. The star symbol denotes the center of the hypersphere, the solid triangle denotes the sampled examples, and the dotted triangle denotes other examples in the whole dataset. The solid green line denotes the distance from a data embedding to the hypersphere’s surface. The left part illustrates the initialization stage, where the sampled data estimate the center and radius, and the right part illustrates the learning stage, where the center and radius are simultaneously optimized.

where $d : \mathbb{R}^D \times \mathbb{R}^D \rightarrow [0, +\infty)$ is the distance function in the metric space. f_ϕ is a neural encoder parameterized by ϕ , while z and ϵ denote the center and the radius of the hypersphere. We use $\mathcal{M}(\cdot)$ to denote the measurement between a data point and a hypersphere prototype based on $d(\cdot)$.

The central idea is to learn a hypersphere prototype for each class with limited episodic supervision, and each example in the query set (x^*, y^*) is predicted by the measurement to the hypersphere prototypes $\mathcal{M}(x_j^*, \mathcal{B}^d)$, which is the Euclidean distance from the embedding to the *surface* of the hyperspheres,

$$\mathcal{M}(x, \mathcal{B}) = d(f_\phi(x), z) - \epsilon = \|f_\phi(x) - z\|_2^2 - \epsilon. \quad (2)$$

Note that in this case, the value of $\mathcal{M}(\cdot)$ may be negative. That is, geometrically speaking, the point is contained inside the hypersphere, which does not affect the calculation of the loss function and the prediction. Generally, the idea is to use areas instead of points in the embedding space to model prototypes, and hyperspheres naturally have two advantages. First, as stated in § 1, one hypersphere prototype could be uniquely modeled by the center z and the radius ϵ , while characterizing manifolds with complex boundaries in the embedding space is intricate. Second, it is easy to optimize the parameters by conducting metric-based classification since they are naturally involved in measurement calculation. In this geometric interpretation, sparse classes will have larger learned radii, while compact classes will have smaller learned radii.

3.2 Hypersphere Prototypes

To construct hypersphere prototypes, the first step is the initialization of the center z and the radius ϵ of the hypersphere. To start with a reasonable approximation of the data distribution, we randomly select K instances from each class for initialization. Specifically for one class, the center of the hypersphere prototype is the mean output of the K embeddings as the estimation in Snell et al. (2017), and the radius is the mean of the distance of each sample to the center. \mathcal{S}_n is the set of sampled instances from the n -th class,

$$\mathcal{B}_n := \begin{cases} z_n = \frac{1}{K} \sum_{x \in \mathcal{S}_n} f_\phi(x), \\ \epsilon_n = \frac{1}{K} \sum_{x \in \mathcal{S}_n} d(f_\phi(x), z_n). \end{cases} \quad (3)$$

Once initialized, a hypersphere prototype will participate in the training process, where its center and radius are simultaneously optimized. During training, for each episode, assume the sampled classes are $\mathcal{N} = \{n_1, n_2, \dots, n_N\}$, the probability of one query point $x \in \mathcal{Q}$ belonging to class n is calculated by softmax over the metrics to the corresponding N hypersphere prototypes.

$$p(y = n | x; \phi) = \frac{\exp(-\mathcal{M}(x, \mathcal{B}_n))}{\sum_{n' \in \mathcal{N}} \exp(-\mathcal{M}(x, \mathcal{B}_{n'}))}. \quad (4)$$

And the parameters of f and hypersphere prototypes are optimized by minimizing the metric-based cross-entropy objective:

$$\mathcal{L}_{\text{cls}} = -\log p(y | x, \phi, z, \epsilon). \quad (5)$$

Equation 4 explains the combination of the advantages of hypersphere prototypes, where \mathcal{M} is calculated by r and z , which will participate in the optimization. The parameters of the neural network ϕ are optimized along with the centers and radii of hypersphere prototypes through gradient descent. To sum up, in the initialization stage, the hypersphere prototypes of all classes in the training set, which are parameterized by z and ϵ , are estimated by the embeddings of randomly selected instances and *stored* for subsequent training and optimization. In the learning stage, the stored ϵ is optimized by an independent optimizer, because, empirically, the parameter could benefit from large learning rates. The optimization will yield a final location and size of the hyperspheres to serve the classification performance. More importantly, the involvement of prototype centers and radii in the training process will, in turn, affect the optimization of encoder parameters, stimulating more expressive and distinguishable representations.

Algorithm 1 expresses the initialization and learning stages of hypersphere prototypes. Although the centers and radii are stored and optimized continuously in training (in contrast with vanilla prototypes where centers are re-estimated at each episode), the whole process is still largely episodic, as in each episode, the samples in the query set are only evaluated against the classes in that single episode instead of the global training class set.

Meanwhile, a standard episodic evaluation process is adopted to handle the unseen classes, where we estimate prototype centers and radii in closed forms. In the episodic evaluation procedure, HyperProto directly takes the mean of instance embeddings as the centers and the mean distance of each instance to the center as the radius (as in Equation 3), following previous standard (Vinyals et al., 2016; Snell et al., 2017; Zhang et al., 2020a).

3.3 Generalizations

We have introduced the mechanisms of hypersphere prototypes in Euclidean space. In this section, we generalize this idea to construct variants with other measurements.

Cone-like Prototypes. Cosine similarity is a commonly used measurement in machine learning. Assume all the data points are distributed on a unit ball, and we use the cosine of the angle to measure the similarity of the two embeddings.

While keeping the intuition of the modeling of hypersphere prototypes in mind, we introduce an additional angle parameter ϵ . We use $\theta_{a,b}$ to denote the angle of the two embeddings a and b . In this way, the center point z and the angle ϵ could jointly construct a cone-like prototype,

$$\mathcal{B}^d(z, f_\phi, \epsilon) := \{f_\phi(x) \in \mathbb{R}^D : d(f_\phi(x), z) \geq \cos \epsilon\}, \quad (6)$$

where $d(f_\phi(x), z) = \cos(\theta_{f_\phi(x), z})$. The measurement $\mathcal{M}(\cdot)$ is defined as the cosine of the angle between the instance embedding and the nearest point on the border of the prototype,

$$\mathcal{M}(x, \mathcal{B}) = \begin{cases} -\cos(\theta_{f_\phi(x), z} - \epsilon), & \theta_{f_\phi(x), z} \geq |\epsilon|, \\ -1, & \theta_{f_\phi(x), z} < |\epsilon|. \end{cases} \quad (7)$$

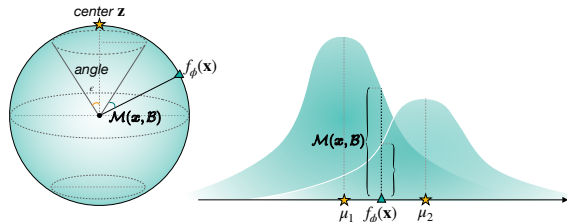


Figure 2: Two variants according to different measurements. The left is the cone-like modeling with cosine similarities, and the right is the Gaussian modeling from the probability perspective.

Similar to the vanilla hypersphere prototypes, z and ϵ need to participate in the learning process for optimization, and the angle $\theta_{x,z}$ is computed by the inverse trigonometric function,

$$\theta_{f_\phi(x), z} = \arccos \frac{f_\phi(x)^T z}{\|f_\phi(x)\| \cdot \|z\|}. \quad (8)$$

The prediction for a training example is also based on the softmax over the measurements to the prototypes like Eq. 5. Note that as shown in Eq. 7, the measurement becomes -1 when a data point is “inside” the cone-like prototype. Then it is hard to make a prediction when an embedding is inside two prototypes. It thus requires that the prototypes do not intersect with each other, that is, to guarantee the angle between two center points is larger than the sum of their own parameter angles,

$$\mathcal{L}_{\text{dis}} = \frac{1}{N} \sum_{i,j} \max(|\epsilon_i| + |\epsilon_j| - \theta_{z_i, z_j}, 0). \quad (9)$$

Therefore, the final loss function is $\mathcal{L} = \mathcal{L}_{\text{cls}} + \mathcal{L}_{\text{dis}}$.

Algorithm 1: Training process. f_ϕ is the feature encoder, N_{total} is the total number of classes in the training set, N is the number of classes for support and query set, K is the number of examples per class in the support set, K' is the number of examples per class in the query set, M is a hyper-parameter. $\text{RANDOMSAMPLE}(S, K)$ denotes a set of K elements chosen uniformly at random from set S , without replacement. λ_f and λ_ϵ are separate learning rates.

Input: Training data $\mathcal{D}_{\text{train}} = \{(\mathbf{x}_1, y_1), \dots, (\mathbf{x}_T, y_T)\}$, $y_i \in \{1, \dots, N_{\text{total}}\}$. \mathcal{D}_k denotes the subset of \mathcal{D} containing all elements (\mathbf{x}_i, y_i) such that $y_i = k$

Output: The updated encoder f_ϕ

// Initialization phase

for $n = 1$ to N_{total} **do**

$\mathcal{S}_n \leftarrow \text{RANDOMSAMPLE}(\mathcal{D}_n, K)$
 $\mathbf{z}_n \leftarrow \frac{1}{|\mathcal{S}_n|} \sum_{(\mathbf{x}_i, y_i) \in \mathcal{S}_n} f_\phi(\mathbf{x}_i)$,
 $\epsilon_n \leftarrow \frac{1}{|\mathcal{S}_n|} \sum_{(\mathbf{x}_i, y_i) \in \mathcal{S}_n} d(f_\phi(\mathbf{x}_i), \mathbf{z}_n)$,

// Learning phase

for $i = 1$ to M **do**

$V \leftarrow \text{RANDOMSAMPLE}(\{1, \dots, N_{\text{total}}\}, N)$, $\mathcal{L}_{\text{cls}} \leftarrow 0$

for n in $\{1, \dots, N\}$ **do**

$\mathcal{Q}_n \leftarrow \text{RANDOMSAMPLE}(\mathcal{D}_{V_n}, K')$
 $\mathcal{L}_{\text{cls}} \leftarrow \mathcal{L}_{\text{cls}} + \frac{1}{NK'} \sum_{(\mathbf{x}_i, y_i) \in \mathcal{Q}_n} [d(f_\phi(\mathbf{x}_i), \mathbf{z}_n) - \epsilon_n + \log \sum_{n'} \exp(\epsilon_{n'} - d(f_\phi(\mathbf{x}_i), \mathbf{z}_{n'}))]$

UPDATE \mathbf{z} , ϵ , f_ϕ w.r.t \mathcal{L}_{cls} , λ_f , λ_ϵ

Gaussian Prototypes. From the probability perspective, each class can be characterized by a distribution in a multi-dimensional feature space. The measurement of a query sample to the n -th class can thus be represented by the negative log likelihood of $f_\phi(\mathbf{x})$ belonging to \mathcal{B}_n . In line with other works (Zhang et al., 2019; Li et al., 2020d), we can simply assume each class subjects to a Gaussian distribution $\mathcal{B}_n \sim \mathcal{N}(\boldsymbol{\mu}_n, \Sigma_n)$. To reduce the number of parameters and better guarantee the positive semi-definite feature, we can further restrict the covariance matrix to be a diagonal matrix such that $\Sigma_n = \sigma_n^2 I$. Then the measurement becomes

$$\begin{aligned} \mathcal{M}(\mathbf{x}, \mathcal{B}_n) &= -\log p(f_\phi(\mathbf{x}); \mathcal{B}_n) \\ &= \frac{\|f_\phi(\mathbf{x}) - \boldsymbol{\mu}_n\|_2^2}{2\sigma_n^2} + \log((2\pi)^{\frac{d}{2}} |\sigma_n|^d) \quad (10) \\ &= \frac{\|f_\phi(\mathbf{x}) - \boldsymbol{\mu}_n\|_2^2}{2\sigma_n^2} + d \log |\sigma_n| + \delta, \end{aligned}$$

where $\delta = \frac{d}{2} \log 2\pi$. The probability of target class given a query sample can be calculated by Eq. 4 in the same fashion: $p(y = n|\mathbf{x}) = \frac{p(f_\phi(\mathbf{x}); \mathcal{B}_n)}{\sum_{n'} p(f_\phi(\mathbf{x}); \mathcal{B}_{n'})}$. Note that the derived form of the equation is the same as directly calculating the probability of $p(y = n|\mathbf{x})$ under a uniform prior distribution of $p(y)$. Comparing with pure probabilistic

approaches, such as variational inference that treats \mathcal{B} as hidden variables and models $p(\mathcal{B}|\mathcal{S})$ and $p(\mathcal{B}|\mathcal{S}, \mathbf{x})$ with neural network (Zhang et al., 2019), under the framework of § 3.2, θ is explicitly parameterized and optimized for each class during training. Moreover, comparing Eq. 10 with Eq. 2, it can be observed that when formalizing \mathcal{B} as a distribution, instead of as a bias term, the original radius parameter (now the variance) functions as a scaling factor on Euclidean distance.

4 Experiments

To evaluate the effectiveness of the proposed method, we conduct experiments on three few-shot learning tasks in NLP and CV, including few-shot named entity recognition (NER), few-shot relation extraction (RE), and few-shot image classification. We chose these three tasks because they all have well-established datasets and baselines to facilitate comprehensive comparisons, while they are still challenging under the few-shot setting as fundamental tasks in NLP and CV. Apart from the experimental study in this section, additional experiments and analyses are reported in Appendix A. The task descriptions, datasets, and implementation details are reported in Appendix B.

Techniques like the structures of neural models, task-specific pre-training, and distillation are *orthogonal* to our contributions.

4.1 Comparison with Embedding Prototypes

We first investigate the direct effect of the proposed geometrical modeling on few-shot learning. We choose the vanilla modeling of prototypes, i.e., using vectors with the same dimension of hidden representations, as our primary baseline. As illustrated in Figure 3, our method consistently outperforms vanilla prototypes on all the tasks. Specifically for named entity recognition, our method yield an increase of at least 5% in f1-score across all settings; for relation extraction, our method achieves improvements of 3% ~ 19% in f1-score across all settings; for image classification, the improvements are range from 2% ~ 4%. Since all other settings in this experiment are identical, the results could directly demonstrate the superiority of hypersphere modeling.

4.2 Comparison with Other Approaches

Few-shot Named Entity Recognition. Table 1 shows the performance of other methods on FEW-NERD. Overall, `HyperProto` has a considerable advantage over vanilla `ProtoNet`, with an increase of at least 5% in f1-score across all settings. The success on both datasets demonstrates that `HyperProto` can learn the general distribution pattern of entities across different classes and thus can greatly improve the performance when little information is shared between the training and test set. It can also be observed that a large portion of the improvement comes from the increase in precision, indicating the ability of `HyperProto` to distinguish entities from context. It is possibly because context words are very diverse, and modeling them with a hypersphere as prototypes is more fitting than a single point as in `ProtoNet`. With respect to the number of shots, `HyperProto` is more advantageous when larger shots are provided and becomes the new state-of-art in the 5~10 shot setting. For the comparison with `NNShot`, `HyperProto` remains superior under the settings of high-shot (5~10), outperforming it by at least 10% of the F1 score. Interestingly, the performances of `NNShot` and `HyperProto` are comparable when it comes to low-shot. This is probably because, in the sequence labeling task, it is more difficult to infer the class-level information from very

limited tokens. In this case, the modeling ability of hypersphere prototypes degenerates towards the nearest-neighbors strategy in `NNShot`. As the shot number increases, the memory cost of `NNShot` grows quadratically and becomes unaffordable, while `HyperProto` keeps it in reasonable magnitude. In this sense, `HyperProto` is more efficient. We also believe a carefully designed initialization strategy is vital for the performance of our model in low-shot settings. The impact of the number of shots is reported in Appendix A.2.

Few-shot Relation Extraction. Table 2 presents the results on two `FewRel` tasks. Methods that use additional data or conduct task-specific encoder pre-training are not included. `HyperProto` generally performs better than all baselines across all settings. In terms of backbone models, when combined with pre-trained models like BERT, hypersphere prototypes can yield a larger advantage against prototypes. It shows that the hypersphere modeling of prototypes can better approximate the real data distribution and boosts the finetuning of BERT. Meanwhile, it sheds light on the untapped ability of large pre-trained language models and stresses that a proper assumption about data distribution may help us unlock the potential. `HyperProto`'s outstanding performance on the Domain Adaptation task further validates the importance of a better abstraction of data in transfer learning. Meanwhile, the large performance variation in the domain adaptation task suggests that when the domain shifts, the estimation of hypersphere prototypes becomes less stable.

To further evaluate the compatibility of our approach and other orthogonal techniques, we conduct task-specific pre-training for relation extraction, where 1,000,000 instances are collected as the training data in a distantly supervised manner from Wikipedia. In the data-collecting process, we ensure that no instances from `FewRel` and `FewRel 2.0` are involved. Then we directly train a BERT encoder with the naive cross-entropy objective function to obtain the final encoder. It could be observed that, with this pre-trained encoder, the performance of our method boosts substantially, demonstrating the model-agnostic nature of our approach.

Few-shot Image Classification. Table 3 shows the result on `miniImageNet` few-shot classification under 2 settings. `HyperProto` substantially outperforms the primary baselines in most settings, displaying their ability to model the class distribu-

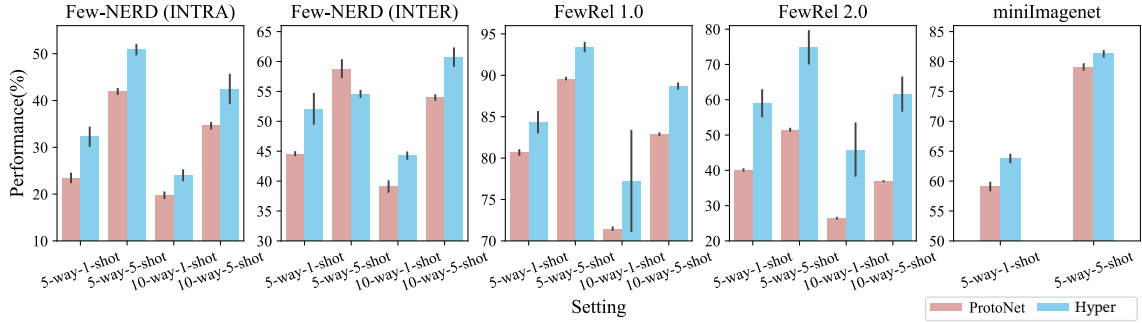


Figure 3: Performance comparison between vanilla prototypes and our hypersphere prototypes, we use the same BERT model as the encoder for all experiments in named entity recognition and relation extraction.

Setting	Eva.	FEW-NERD (INTRA)			FEW-NERD (INTER)		
		NNShot	ProtoNet	HyperProto	NNShot	ProtoNet	HyperProto
5 way 1~2 shot	P	28.95 ± 1.02	18.58 ± 1.02	40.18 ± 1.71	50.40 ± 0.60	38.70 ± 0.50	53.36 ± 2.74
	R	33.40 ± 1.44	31.83 ± 1.03	26.96 ± 2.07	58.84 ± 0.13	52.60 ± 1.65	51.12 ± 4.94
	F	31.01 ± 1.21	23.45 ± 0.92	32.26 ± 1.94	54.29 ± 0.40	44.58 ± 0.26	52.09 ± 2.49
5 way 5~10 shot	P	32.87 ± 2.45	35.87 ± 0.69	48.77 ± 0.79	45.80 ± 3.53	53.73 ± 1.77	62.26 ± 0.89
	R	39.17 ± 2.17	50.50 ± 1.88	53.26 ± 2.60	56.45 ± 2.93	64.99 ± 2.24	69.32 ± 1.66
	F	35.74 ± 2.36	41.93 ± 0.55	50.88 ± 1.01	50.56 ± 3.33	58.80 ± 1.42	65.59 ± 0.50
10 way 1~2 shot	P	20.38 ± 0.22	16.52 ± 0.52	26.06 ± 2.40	42.74 ± 2.05	32.59 ± 0.22	45.38 ± 0.49
	R	23.63 ± 0.53	24.60 ± 0.72	22.32 ± 0.54	52.16 ± 1.76	48.91 ± 2.94	43.22 ± 1.33
	F	21.88 ± 0.23	19.76 ± 0.59	24.02 ± 1.06	46.98 ± 1.96	39.09 ± 0.87	44.26 ± 0.53
10 way 5~10 shot	P	25.46 ± 0.63	28.93 ± 0.82	38.94 ± 3.39	45.15 ± 0.81	47.93 ± 0.45	56.38 ± 1.79
	R	30.32 ± 1.71	43.08 ± 0.84	46.71 ± 2.48	56.05 ± 0.37	61.79 ± 1.73	65.84 ± 1.61
	F	27.67 ± 1.06	34.61 ± 0.59	42.46 ± 3.04	50.00 ± 0.36	53.97 ± 0.38	60.73 ± 1.47
Average	F	29.08	29.94	37.41	50.46	49.11	55.66

Table 1: Performance on the FEW-NERD dataset. P denotes precision, R denotes recall, and F refers to the F1 score. The standard deviation is reported with 3 runs with different random seeds for each model.

tion of images. We observe that compared to NLP, image classification results are more stable both for vanilla prototypes and hypersphere prototypes. This observation may indicate the difference in encoding between the two technologies. Token representations in BERT are contextualized and changeable around different contexts, yet the image representation produced by deep CNNs aims to capture the global and local features thoroughly. Under the 5-way 5-shot setting, the improvements of HyperProto are significant. The effectiveness of our method is also demonstrated by the comparisons with other previous few-shot learning methods with the same backbones. In particular, HyperProto yields the best results of all the compared methods with the WideResNet (Zagoruyko and Komodakis, 2016) backbone, suggesting that the expressive capability of hypersphere prototypes can be enhanced with a more

powerful encoder. Compared to the 5-shot setting, our model improves mediocly in the 1-shot setting of ConvNet and ResNet-12 (He et al., 2015). The phenomenon is consistent with the intuition that more examples would be more favorable to the learning of radius. We further analyze the dynamics of the radius of our method in Appendix 4.4.

4.3 Experimental Analysis

Comparison of Generalized Prototypes. To further compare the variants of our approach, we conduct experiments for cone-like and gaussian prototypes with WideResNet-28-10 on miniImageNet as well. Table 4 presents results across three measurement settings. Although the two variants do not perform better than our main method, they still considerably outperform many baselines in Table 3. While the three models’ performance is close under the 1-shot setting, the cone-like prototypes model

Model	FewRel 1.0				
	5 way 1 shot	5 way 5 shot	10 way 1 shot	10 way 5 shot	Average
Meta Net (Munkhdalai and Yu, 2017)	64.46 ± 0.54	80.57 ± 0.48	53.96 ± 0.56	69.23 ± 0.52	67.06
SNAIL (Mishra et al., 2017)	67.29 ± 0.26	79.40 ± 0.22	53.28 ± 0.27	68.33 ± 0.26	67.08
GNN CNN (Satorras and Estrach, 2018)	66.23 ± 0.75	81.28 ± 0.62	46.27 ± 0.80	64.02 ± 0.77	64.45
GNN BERT (Satorras and Estrach, 2018)	75.66 ± 0.00	89.06 ± 0.00	70.08 ± 0.00	76.93 ± 0.00	77.93
Proto-HATT (Gao et al., 2019a)	76.30 ± 0.06	90.12 ± 0.04	64.13 ± 0.03	83.05 ± 0.05	78.40
MLMAN (Ye and Ling, 2019)	82.98 ± 0.20	92.66 ± 0.09	73.59 ± 0.26	87.29 ± 0.15	84.13
MTB (Soares et al., 2019)	89.80	93.59	83.37	88.64	88.85
REGRAB (Qu et al., 2020)	90.30	94.25	84.09	89.93	89.64
ProtoCNN	69.20 ± 0.20	84.79 ± 0.16	56.44 ± 0.22	75.55 ± 0.19	71.50
HyperProto CNN (Ours)	66.05 ± 3.44	87.31 ± 0.93	56.74 ± 1.06	77.87 ± 2.60	71.99
ProtoBERT	80.68 ± 0.28	89.60 ± 0.09	71.48 ± 0.15	82.89 ± 0.11	81.16
HyperProto BERT (Ours)	84.34 ± 1.23	93.42 ± 0.50	77.24 ± 6.05	88.71 ± 0.31	85.93
HyperProto BERT+Pretrain (Ours)	89.90 ± 0.43	96.23 ± 0.21	83.55 ± 0.59	92.90 ± 0.19	90.65
FewRel 2.0 Domain Adaptation					
Proto-ADV CNN (Wang et al., 2018)	42.21 ± 0.09	58.71 ± 0.06	28.91 ± 0.10	44.35 ± 0.09	43.55
Proto-ADV BERT (Gao et al., 2019b)	41.90 ± 0.44	54.74 ± 0.22	27.36 ± 0.50	37.40 ± 0.36	40.35
BERT-pair (Gao et al., 2019b)	56.25 ± 0.40	67.44 ± 0.54	43.64 ± 0.46	53.17 ± 0.09	55.13
ProtoCNN	35.09 ± 0.10	49.37 ± 0.10	22.98 ± 0.05	35.22 ± 0.06	35.67
HyperProto CNN (Ours)	36.41 ± 1.43	55.50 ± 1.42	22.11 ± 0.58	40.82 ± 2.50	38.71
ProtoBERT	40.12 ± 0.19	51.50 ± 0.29	26.45 ± 0.10	36.93 ± 0.01	38.75
HyperProto BERT (Ours)	59.03 ± 3.68	74.85 ± 4.59	45.88 ± 7.43	61.61 ± 4.69	60.34
HyperProto BERT+Pretrain (Ours)	73.98 ± 1.72	90.06 ± 0.45	61.42 ± 0.79	81.39 ± 1.25	76.71

Table 2: Accuracies on FewRel 1.0 and FewRel 2.0 under 4 different settings. The standard deviation is reported with 3 runs with different random seeds for each model.

Model	Backbone	<i>miniImageNet</i>	
		5 way 1 shot	5 way 5 shot
Infinite Mixture Prototypes (Allen et al., 2019)	ConvNet	33.30 ± 0.71	65.88 ± 0.71
ProtoNet (Snell et al., 2017)	ConvNet	46.44 ± 0.60	63.72 ± 0.55
CovaMNet (Li et al., 2019a)	ConvNet	51.83 ± 0.64	65.65 ± 0.77
HyperProto (Ours)	ConvNet	50.21 ± 0.31	66.48 ± 0.71
SNAIL (Mishra et al., 2017)	ResNet-12	55.71 ± 0.99	68.88 ± 0.92
ProtoNet (Snell et al., 2017)	ResNet-12	53.81 ± 0.23	75.68 ± 0.17
Variational FSL (Zhang et al., 2019)	ResNet-12	61.23 ± 0.26	77.69 ± 0.17
Prototypes + TRAML (Li et al., 2020a)	ResNet-12	60.31 ± 0.48	77.94 ± 0.57
HyperProto (Ours)	ResNet-12	59.65 ± 0.62	78.24 ± 0.47
ProtoNet (Snell et al., 2017)	WideResNet-28-10	59.09 ± 0.64	79.09 ± 0.46
Activation to Parameter (Qiao et al., 2018)	WideResNet-28-10	59.60 ± 0.41	73.74 ± 0.19
LEO (Rusu et al., 2018)	WideResNet-28-10	61.76 ± 0.08	77.59 ± 0.12
SimpleShot (Wang et al., 2019)	WideResNet-28-10	63.50 ± 0.20	80.33 ± 0.14
AWGIM (Guo and Cheung, 2020)	WideResNet-28-10	63.12 ± 0.08	78.40 ± 0.11
HyperProto (Ours)	WideResNet-28-10	63.78 ± 0.63	81.29 ± 0.46

Table 3: Accuracies with 95% confidence interval on 1000 test episodes of HyperProto and baselines on *miniImageNet*.

performs worse in the 5-shot setting. It could be attributed to unsatisfying radius learning. It is found that the cone-like prototypes model is susceptible to radius learning rate and is prone to overfitting.

Cross-dataset Few-shot Learning. We also conduct experiments on the more difficult cross-dataset setting. Specifically, the model trained on *miniImageNet* is tested on the CUB dataset (Welin-

Methods	<i>miniImageNet</i>	
	5 way 1 shot	5 way 5 shot
Cone HyperProto	62.43 ± 0.63	76.03 ± 0.50
Gaussian HyperProto	60.34 ± 0.64	80.43 ± 0.45
HyperProto	63.78 ± 0.63	81.29 ± 0.46

Table 4: Accuracies with 95% confidence interval of generalized HyperProto on *miniImageNet*.

Methods	Backbone	5 way 5 shot
	<i>miniImageNet</i> → CUB	
MatchingNet (Vinyals et al., 2016)	RN-12	53.07 ± 0.74
ProtoNet (Snell et al., 2017)	RN-12	62.02 ± 0.70
MAML (Finn et al., 2017)	RN-18	52.34 ± 0.72
RelationNet (Sung et al., 2018)	RN-18	57.71 ± 0.73
Baseline++ (Chen et al., 2021)	RN-18	62.04 ± 0.76
SimpleShot (Wang et al., 2019)	RN-18	65.56 ± 0.70
HyperProto (Ours)	RN-12	63.22 ± 0.77

Table 5: Results on cross-dataset classification.

der et al., 2010) under the 5-way 5-shot setting. We use ResNet-12 (RN-12) (He et al., 2015) as the backbone in our experiment. Table 5 shows the results compared with several baselines. It can be seen that HyperProto outperforms the baselines by a large margin even with less powerful encoder (RN-12), indicating the ability to learn representations that are transferrable to new domains. The results also echo the performance of HyperProto for the cross-domain relation extraction in Table 2.

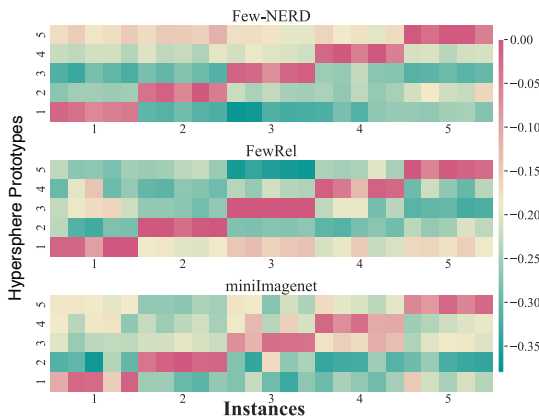


Figure 4: Normalized distances from instances to hypersphere prototypes. Horizontal axis: hypersphere prototypes of 5 classes. Vertical axis: 5 instances per class.

Representation Analysis. To study if the learned representations are discriminative, we illustrate the normalized distances between the learned represen-

tations and the hypersphere prototypes in Figure 4. Specifically, we randomly sample 5 classes and 25 instances (5 per class) for each dataset and produce representations for the instances and hypersphere prototypes for the classes. Then, we calculate the distance between each instance to each prototype (i.e., distance from the point to the hypersphere surface) to produce the matrix. All the values in the illustration are normalized since the absolute values may vary with the datasets. Warmer colors denote shorter distances in the illustration. The illustration shows that in all three datasets, our model could effectively learn discriminative representations and achieve stable metric-based classification. In order to further analyze the representations produced by HyperProto, we study the similarities of randomly sampled instance embeddings. We randomly select 4×5 classes and 5 instances per class in FEW-NERD, FewRel and *miniImageNet*, respectively. As illustrated in Figure 5, each subfigure is a 25×25 matrix based on 5 classes. We calculate the cosine similarities of these embeddings and observe clear intra-class similarity and inter-class distinctiveness. This result confirms the robustness of our model since all the classes and instances are sampled randomly.

4.4 Analysis of the Radius Dynamics

In this section, the mechanism of hypersphere prototypes will be empirically analyzed. We demonstrate the mechanism of hypersphere prototypes by illustrating the change of radius for one specific hypersphere. In the learning phase, the radius of a hypersphere prototype is changing according to the “density” of the sampled episode, which could be characterized by the mean distance of samples to the corresponding prototype center. Practically, due to randomness in sampling, the value of the mean distance may oscillate at a high frequency in this process, and the radius changes accordingly. To better visualize the changing of radius along with the mean distance at each update, for each round of training, we fix one specific class as the *anchor class* for mean distance and radius recording and apply a special sampling strategy at each episode. Specifically, we take FewRel training data and train on the 5 way 5 shot setting with CNN encoder. While training, each episode contains the *anchor class* and 4 other randomly sampled classes. Training accuracy is logged every 50 steps. After a warmup training of 500 steps, we sample

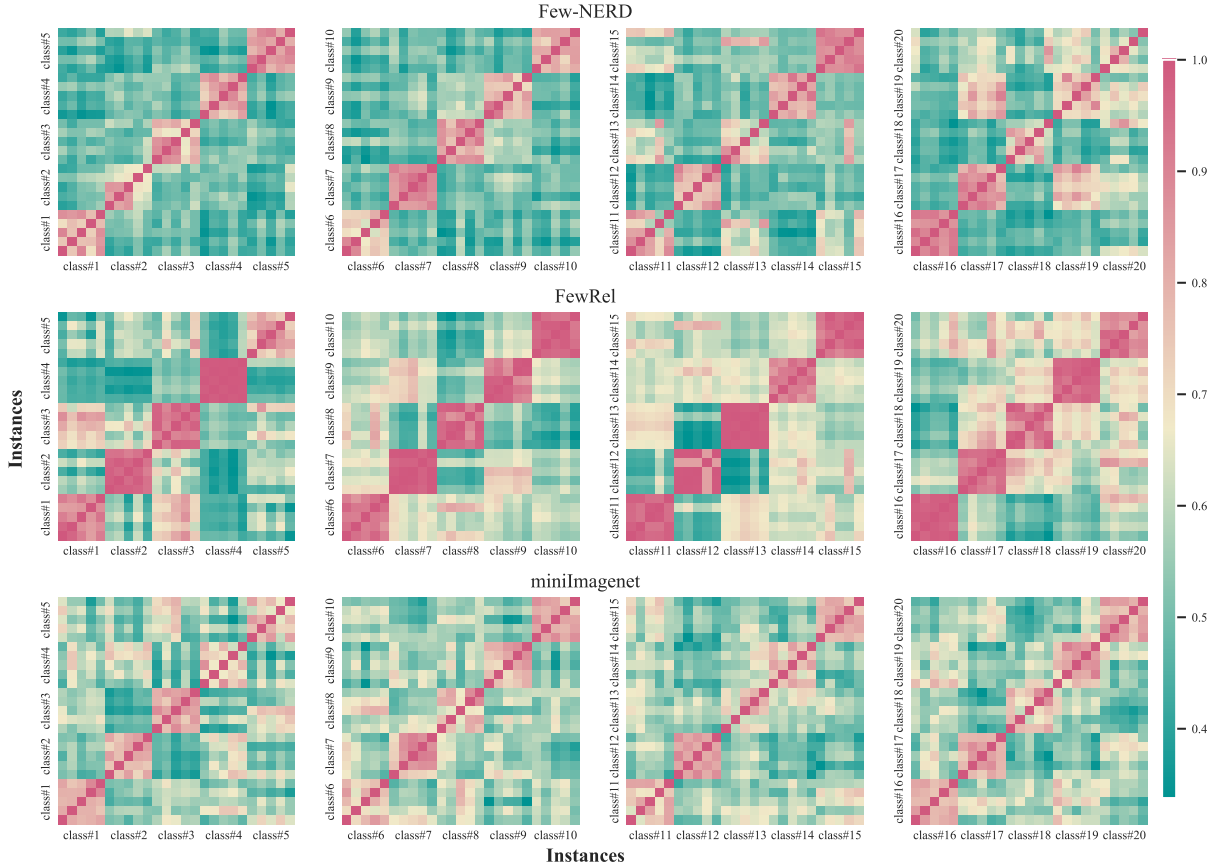


Figure 5: Representation similarity matrix produced by HyperProto on FEW-NERD, FewRel and *miniImageNet*. Each row illustrates 20 classes and 100 instances in one dataset. Each subfigure contains 5 classes and 25 instances. Each unit denotes the cosine similarity of two embeddings, and each 5×5 cell indicates the comparison of two classes. The units on the diagonal represent the same instance, and the 5×5 cells on the diagonal represent the same class. Warmer color means higher similarity in this illustration.

“good” or “bad” episodes for every 50 steps alternatively. A “good” episode has higher accuracy on the anchor class than the previously logged accuracy, while conversely, a “bad” episode has an accuracy lower than before. The mean distance to the prototype center and radius at each episode are logged every 50 steps after the warmup. Figure 6 shows the changing of mean distance and radius for 8 classes during 600~2000 training steps. Although the numeric values of distance and radius differ greatly and oscillate at different scales, they have similar changing patterns. Besides, it could be observed that there is often a small time lag in the change of radius, indicating that the change of radius is brought by the change in mean distance. This is in line with our expectations and perfectly demonstrates the learning mechanism of hypersphere prototypes. The experiment provides a promising idea, if we can control the sampling strategy through knowledge a priori, we may find a

way to learn ideal hypersphere prototypes.

5 Related Work

This work is related to studies of meta-learning, whose primary goal is to quickly adapt deep neural models to new tasks with a few training examples (Hospedales et al., 2020). To this end, two branches of studies are proposed: optimization-based methods and metric-based methods. The optimization-based studies (Finn et al., 2017; Franceschi et al., 2018; Ravi and Beatson, 2018) regard few-shot learning as a bi-level optimization process, where a global optimization is conducted to learn a good initialization across various tasks, and a local optimization quickly adapts the initialization parameters to specific tasks by a few steps of gradient descent.

Compared to the mentioned studies, our work is more related to the metric-based meta-learning approaches (Vinyals et al., 2016; Snell et al., 2017;

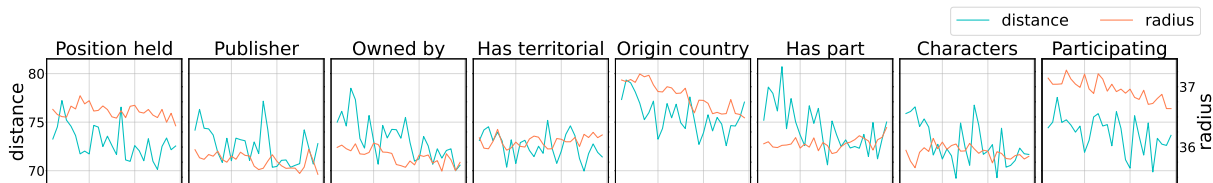


Figure 6: The illustration depicts the radius change according to the degree of sparsity of the sampled episode. Each subfigure represents a selected anchor class in the FewRel dataset. The horizontal axis represents the increase of training steps.

Satorras and Estrach, 2018; Sung et al., 2018), whose general idea is to learn to measure the similarity between representations and find the closest labeled example (or a derived prototype) for an unlabeled example. Typically, these methods learn a measurement function during episodic optimization. More specifically, we inherit the spirit of using prototypes to abstractly represent class-level information, which could be traced back to cognitive science (Reed, 1972; Rosch et al., 1976; Nosofsky, 1986), statistical machine learning (Graf et al., 2009) and to the Nearest Mean Classifier (Mensink et al., 2013). In the area of deep learning, Snell et al. (2017) propose the prototypical network to exploit the average of example embeddings as a prototype to perform metric-based classification in few-shot learning. In their work, prototypes are estimated by the embeddings of instances. However, it is difficult to find a satisfying location for the prototypes based on the entire dataset. Ren et al. (2018) adapt such prototype-based networks in the semi-supervised scenario where the dataset is partially annotated. Moreover, a set of prototype-based networks are proposed concentrating on the improvements of prototype estimations and application to various downstream tasks (Allen et al., 2019; Gao et al., 2019a; Li et al., 2019b; Pan et al., 2019; Seth et al., 2019; Ding et al., 2021b; Li et al., 2020c; Wertheimer and Har- iharan, 2019; Xie et al., 2022; Zhang et al., 2020a). We discuss our method within the context of other prototype-enhanced methods in Appendix C.1. There has also been a growing body of work that considers the few-shot problem from multiple perspectives, bringing new thinking to the field (Tian et al., 2020; Yang et al., 2021; Laenen and Bertinetto, 2021; Zhang et al., 2020b; Wang et al., 2021; Das et al., 2021; Wertheimer et al., 2021; Ding et al., 2021a; Cui et al., 2022; Hu et al., 2022).

There has also been a series of works that embed prototypes into a non-Euclidean out-

put space (Mettes et al., 2019; Keller-Ressel, 2020; Atigh et al., 2021). It should be noted that these studies regard hyperspheres or other non-Euclidean manifolds as a characterization of the embedding space, while our proposed method use hyperspheres to represent prototypes and conduct metric-based classification in the Euclidean space. Therefore, the focus of our proposed HyperProto is different from the above non-Euclidean prototype-based works.

6 Conclusion

This paper proposes a novel metric-based few-shot learning method, *hypersphere prototypes*. Unlike previous metric-based methods that use dense vectors to represent the class-level semantics, we use hyperspheres to enhance the capabilities of prototypes to express the intrinsic information of the data. It is simple to model a hypersphere in the embedding space and conduct metric-based classification in few-shot learning. Our approach is easy to implement and also empirically effective, we observe significant improvements to baselines on three tasks across NLP and CV. We also develop two variants of prototypes in other embedding spaces. For potential future work, such modeling could be extended to more generalized representation learning like word embeddings.

References

- Kelsey Allen, Evan Shelhamer, Hanul Shin, and Joshua Tenenbaum. 2019. [Infinite mixture prototypes for few-shot learning](#). In *Proceedings of ICML*, pages 232–241. PMLR.
- Mina Ghadimi Atigh, Martin Keller-Ressel, and Pascal Mettes. 2021. [Hyperbolic busemann learning with ideal prototypes](#). *arXiv preprint arXiv:2106.14472*.
- Yinbo Chen, Zhuang Liu, Huijuan Xu, Trevor Darrell, and Xiaolong Wang. 2021. [Meta-baseline: Exploring simple meta-learning for few-shot learning](#). In *Proceedings of the ICCV*, pages 9062–9071.

- Ganqu Cui, Shengding Hu, Ning Ding, Longtao Huang, and Zhiyuan Liu. 2022. Prototypical verbalizer for prompt-based few-shot tuning. In *ACL*.
- Debasmit Das and C. S. George Lee. 2020. A two-stage approach to few-shot learning for image recognition. *IEEE Transactions on Image Processing*, 29:3336–3350.
- Sarkar Snigdha Sarathi Das, Arzoo Katiyar, Rebecca J Passonneau, and Rui Zhang. 2021. Container: Few-shot named entity recognition via contrastive learning. *arXiv preprint arXiv:2109.07589*.
- Cyprien de Lichy, Hadrien Glaude, and William Campbell. 2021. Meta-learning for few-shot named entity recognition. In *Proceedings of the 1st Workshop on Meta Learning of ACL*, pages 44–58.
- Jia Deng, Wei Dong, Richard Socher, Li-Jia Li, Kai Li, and Li Fei-Fei. 2009. Imagenet: A large-scale hierarchical image database. In *Proceedings of CVPR*, pages 248–255.
- Jacob Devlin, Ming-Wei Chang, Kenton Lee, and Kristina Toutanova. 2019. BERT: Pre-training of deep bidirectional transformers for language understanding. In *Proceedings of NAACL*, pages 4171–4186.
- Ning Ding, Yulin Chen, Xu Han, Guangwei Xu, Pengjun Xie, Hai-Tao Zheng, Zhiyuan Liu, Juanzi Li, and Hong-Gee Kim. 2021a. Prompt-learning for fine-grained entity typing. *arXiv preprint arXiv:2108.10604*.
- Ning Ding, Xiaobin Wang, Yao Fu, Guangwei Xu, Rui Wang, Pengjun Xie, Ying Shen, Fei Huang, Hai-Tao Zheng, and Rui Zhang. 2021b. Prototypical representation learning for relation extraction. In *Proceedings of ICLR*.
- Ning Ding, Guangwei Xu, Yulin Chen, Xiaobin Wang, Xu Han, Pengjun Xie, Haitao Zheng, and Zhiyuan Liu. 2021c. Few-NERD: A few-shot named entity recognition dataset. In *Proceedings of ACL*, page 3198–3213.
- Chelsea Finn, Pieter Abbeel, and Sergey Levine. 2017. Model-agnostic meta-learning for fast adaptation of deep networks. In *Proceedings of ICML*, pages 1126–1135.
- Luca Franceschi, Paolo Frasconi, Saverio Salzo, Riccardo Grazi, and Massimiliano Pontil. 2018. Bilevel programming for hyperparameter optimization and meta-learning. In *Proceedings of ICML*, pages 1568–1577.
- Tianyu Gao, Xu Han, Zhiyuan Liu, and Maosong Sun. 2019a. Hybrid attention-based prototypical networks for noisy few-shot relation classification. In *Proceedings of AAAI*, pages 6407–6414.
- Tianyu Gao, Xu Han, Hao Zhu, Zhiyuan Liu, Peng Li, Maosong Sun, and Jie Zhou. 2019b. FewRel 2.0: Towards more challenging few-shot relation classification. In *Proceedings of EMNLP*.
- Arnulf BA Graf, Olivier Bousquet, Gunnar Rätsch, and Bernhard Schölkopf. 2009. Prototype classification: Insights from machine learning. *Neural computation*, pages 272–300.
- Yiluan Guo and Ngai-Man Cheung. 2020. Attentive weights generation for few shot learning via information maximization. In *Proceedings of the IEEE/CVF Conference on Computer Vision and Pattern Recognition*, pages 13499–13508.
- Xu Han, Zhengyan Zhang, Ning Ding, Yuxian Gu, Xiao Liu, Yuqi Huo, Jiezhong Qiu, Liang Zhang, Wentao Han, Minlie Huang, et al. 2021. Pre-trained models: Past, present and future. *AI Open*.
- Xu Han, Hao Zhu, Pengfei Yu, Ziyun Wang, Yuan Yao, Zhiyuan Liu, and Maosong Sun. 2018. FewRel: A large-scale supervised few-shot relation classification dataset with state-of-the-art evaluation. In *Proceedings of EMNLP*, pages 248–255.
- Kaiming He, Xiangyu Zhang, Shaoqing Ren, and Jian Sun. 2015. Deep residual learning for image recognition. In *Proceedings of CVPR*, pages 770–778.
- Timothy Hospedales, Antreas Antoniou, Paul Micaelli, and Amos Storkey. 2020. Meta-learning in neural networks: A survey. *arXiv:2004.05439*.
- Shengding Hu, Ning Ding, Huadong Wang, Zhiyuan Liu, Juan-Zi Li, and Maosong Sun. 2022. Knowledgeable prompt-tuning: Incorporating knowledge into prompt verbalizer for text classification. In *ACL*.
- Jiaxin Huang, Chunyuan Li, Krishan Subudhi, Damien Jose, Shobana Balakrishnan, Weizhu Chen, Baolin Peng, Jianfeng Gao, and Jiawei Han. 2020. Few-shot named entity recognition: A comprehensive study. *arXiv:2012.14978*.
- Sergey Ioffe and Christian Szegedy. 2015. Batch normalization: Accelerating deep network training by reducing internal covariate shift. In *Proceedings of ICML*.
- Martin Keller-Ressel. 2020. A theory of hyperbolic prototype learning. *arXiv preprint arXiv:2010.07744*.
- Diederik P. Kingma and Jimmy Ba. 2017. Adam: A method for stochastic optimization. In *Proceedings of ICLR*.
- Steinar Laenen and Luca Bertinetto. 2021. On episodes, prototypical networks, and few-shot learning. *Advances in Neural Information Processing Systems*, 34.

- Aoxue Li, Weiran Huang, Xu Lan, Jiashi Feng, Zhenguo Li, and Liwei Wang. 2020a. [Boosting few-shot learning with adaptive margin loss](#). In *Proceedings of the CVPR*, pages 12576–12584.
- Jing Li, Billy Chiu, Shanshan Feng, and Hao Wang. 2020b. [Few-shot named entity recognition via meta-learning](#). *IEEE Transactions on Knowledge and Data Engineering*.
- Junnan Li, Pan Zhou, Caiming Xiong, and Steven Hoi. 2020c. [Prototypical contrastive learning of unsupervised representations](#). In *Proceedings of ICLR*.
- Wenbin Li, Lei Wang, Jing Huo, Yinghuan Shi, Yang Gao, and Jiebo Luo. 2020d. [Asymmetric distribution measure for few-shot learning](#). In *Proceedings of IJCAI*, pages 2957–2963.
- Wenbin Li, Jinglin Xu, Jing Huo, Lei Wang, Gao Yang, and Jiebo Luo. 2019a. [Distribution consistency based covariance metric networks for few-shot learning](#). In *AAAI*, pages 8642–8649.
- Xiao Li, Min Fang, Dazheng Feng, Haikun Li, and Jinqiao Wu. 2019b. [Prototype adjustment for zero shot classification](#). *Signal Processing: Image Communication*, pages 242–252.
- Jiang Lu, Pinghua Gong, Jieping Ye, and Changshui Zhang. 2020. [Learning from very few samples: A survey](#). *arXiv:2009.02653*.
- Puneet Mangla, Nupur Kumari, Abhishek Sinha, Mayank Singh, Balaji Krishnamurthy, and Vineeth N Balasubramanian. 2020. [Charting the right manifold: Manifold mixup for few-shot learning](#). In *Proceedings of WACV*, pages 2218–2227.
- Thomas Mensink, Jakob Verbeek, Florent Perronnin, and Gabriela Csurka. 2013. [Distance-based image classification: Generalizing to new classes at near-zero cost](#). *IEEE transactions on pattern analysis and machine intelligence*, pages 2624–2637.
- Pascal Mettes, Elise van der Pol, and Cees Snoek. 2019. [Hyperspherical prototype networks](#). *Proceedings of NeurIPS*, pages 1487–1497.
- Nikhil Mishra, Mostafa Rohaninejad, Xi Chen, and Pieter Abbeel. 2017. [A simple neural attentive meta-learner](#). *arXiv:1707.03141*.
- Tsendsuren Munkhdalai and Hong Yu. 2017. [Meta networks](#). In *International Conference on Machine Learning*, pages 2554–2563. PMLR.
- Robert M Nosofsky. 1986. [Attention, similarity, and the identification–categorization relationship](#). *Journal of experimental psychology: General*.
- Yingwei Pan, Ting Yao, Yehao Li, Yu Wang, Chong-Wah Ngo, and Tao Mei. 2019. [Transferrable prototypical networks for unsupervised domain adaptation](#). In *Proceedings of CVPR*, pages 2239–2247.
- Adam Paszke, Sam Gross, Francisco Massa, Adam Lerer, James Bradbury, Gregory Chanan, Trevor Killeen, Zeming Lin, Natalia Gimelshein, Luca Antiga, et al. 2019. [Pytorch: An imperative style, high-performance deep learning library](#). In *Proceedings of NeurIPS*, pages 8026–8037.
- Siyuan Qiao, Chenxi Liu, Wei Shen, and Alan L Yuille. 2018. [Few-shot image recognition by predicting parameters from activations](#). In *Proceedings of the CVPR*, pages 7229–7238.
- Meng Qu, Tianyu Gao, Louis-Pascal Xhonneux, and Jian Tang. 2020. [Few-shot relation extraction via bayesian meta-learning on relation graphs](#). In *International conference on machine learning*, pages 7867–7876. PMLR.
- Sachin Ravi and Alex Beaton. 2018. [Amortized bayesian meta-learning](#). In *Proceedings of ICLR*.
- Sachin Ravi and Hugo Larochelle. 2017. [Optimization as a model for few-shot learning](#). In *Proceedings of ICLR*.
- Avinash Ravichandran, Rahul Bhotika, and Stefano Soatto. 2019. [Few-shot learning with embedded class models and shot-free meta training](#). In *2019 IEEE/CVF International Conference on Computer Vision, ICCV 2019, Seoul, Korea (South), October 27 - November 2, 2019*, pages 331–339.
- Stephen K Reed. 1972. [Pattern recognition and categorization](#). *Cognitive psychology*, 3(3):382–407.
- Mengye Ren, Eleni Triantafillou, Sachin Ravi, Jake Snell, Kevin Swersky, Joshua B Tenenbaum, Hugo Larochelle, and Richard S Zemel. 2018. [Meta-learning for semi-supervised few-shot classification](#). In *Proceedings of ICLR*.
- Eleanor Rosch, Carolyn B Mervis, Wayne D Gray, David M Johnson, and Penny Boyes-Braem. 1976. [Basic objects in natural categories](#). *Cognitive psychology*, pages 382–439.
- Andrei A Rusu, Dushyant Rao, Jakub Sygnowski, Oriol Vinyals, Razvan Pascanu, Simon Osindero, and Raia Hadsell. 2018. [Meta-learning with latent embedding optimization](#). *arXiv:1807.05960*.
- Victor Garcia Satorras and Joan Bruna Estrach. 2018. [Few-shot learning with graph neural networks](#). In *Proceedings of ICLR*.
- Harshita Seth, Pulkit Kumar, and Muktabh Mayank Srivastava. 2019. [Prototypical metric transfer learning for continuous speech keyword spotting with limited training data](#). In *Proceedings of SOCO*. Springer.
- Jake Snell, Kevin Swersky, and Richard Zemel. 2017. [Prototypical networks for few-shot learning](#). In *Proceedings of NeurIPS*.

- Livio Baldini Soares, Nicholas FitzGerald, Jeffrey Ling, and Tom Kwiatkowski. 2019. Matching the blanks: Distributional similarity for relation learning. In *Proceedings of ACL*.
- Flood Sung, Yongxin Yang, Li Zhang, Tao Xiang, Philip HS Torr, and Timothy M Hospedales. 2018. Learning to compare: Relation network for few-shot learning. In *Proceedings of CVPR*, pages 1199–1208.
- Yonglong Tian, Yue Wang, Dilip Krishnan, Joshua B. Tenenbaum, and Phillip Isola. 2020. Rethinking few-shot image classification: A good embedding is all you need? In *Proceedings of ECCV*, pages 266–282.
- Laurens van der Maaten and Geoffrey Hinton. 2008. Visualizing data using t-sne. *Journal of Machine Learning Research*, 9(86):2579–2605.
- Oriol Vinyals, Charles Blundell, Timothy Lillicrap, Daan Wierstra, et al. 2016. Matching networks for one shot learning. In *Proceedings of NeurIPS*, pages 3630–3638.
- Jixuan Wang, Kuan-Chieh Wang, Frank Rudzicz, and Michael Brudno. 2021. Grad2task: Improved few-shot text classification using gradients for task representation. *Advances in Neural Information Processing Systems*, 34.
- Xiaozhi Wang, Xu Han, Yankai Lin, Zhiyuan Liu, and Maosong Sun. 2018. Adversarial multi-lingual neural relation extraction. In *Proceedings of COLING*, pages 1156–1166.
- Yan Wang, Wei-Lun Chao, Kilian Q Weinberger, and Laurens van der Maaten. 2019. Simpleshot: Revisiting nearest-neighbor classification for few-shot learning. *arXiv:1911.04623*.
- Peter Welinder, Steve Branson, Takeshi Mita, Catherine Wah, Florian Schroff, Serge Belongie, and Pietro Perona. 2010. Caltech-ucsd birds 200.
- Davis Wertheimer and Bharath Hariharan. 2019. Few-shot learning with localization in realistic settings. In *Proceedings of the IEEE/CVF conference on computer vision and pattern recognition*, pages 6558–6567.
- Davis Wertheimer, Luming Tang, and Bharath Hariharan. 2021. Few-shot classification with feature map reconstruction networks. In *Proceedings of the IEEE/CVF Conference on Computer Vision and Pattern Recognition*, pages 8012–8021.
- Thomas Wolf, Lysandre Debut, Victor Sanh, Julien Chaumond, Clement Delangue, Anthony Moi, Pierric Cistac, Tim Rault, Rémi Louf, Morgan Funtowicz, et al. 2020. Huggingface’s transformers: State-of-the-art natural language processing. In *Proceedings of EMNLP: System Demonstrations*, page 38–45.
- Jiangtao Xie, Fei Long, Jiaming Lv, Qilong Wang, and Peihua Li. 2022. Joint distribution matters: Deep brownian distance covariance for few-shot classification. In *Proceedings of the IEEE/CVF Conference on Computer Vision and Pattern Recognition*, pages 7972–7981.
- Shuo Yang, Lu Liu, and Min Xu. 2021. Free lunch for few-shot learning: Distribution calibration. In *Proceedings of ICLR*.
- Yi Yang and Arzoo Katiyar. 2020. Simple and effective few-shot named entity recognition with structured nearest neighbor learning. In *Proceedings of EMNLP*.
- Zhi-Xiu Ye and Zhen-Hua Ling. 2019. Multi-level matching and aggregation network for few-shot relation classification. In *Proceedings of ACL*, pages 2872–2881.
- Sergey Zagoruyko and Nikos Komodakis. 2016. Wide residual networks. In *BMVC*, pages 87.1–87.12.
- Chi Zhang, Yujun Cai, Guosheng Lin, and Chunhua Shen. 2020a. Deepemd: Few-shot image classification with differentiable earth mover’s distance and structured classifiers. In *Proceedings of the IEEE/CVF conference on computer vision and pattern recognition*, pages 12203–12213.
- Jian Zhang, Chenglong Zhao, Bingbing Ni, Minghao Xu, and Xiaokang Yang. 2019. Variational few-shot learning. In *Proceedings of ICCV*, pages 1685–1694.
- Manli Zhang, Jianhong Zhang, Zhiwu Lu, Tao Xiang, Mingyu Ding, and Songfang Huang. 2020b. Iept: Instance-level and episode-level pretext tasks for few-shot learning. In *International Conference on Learning Representations*.

A Additional Experiments and Analysis

This section provides additional experiments and analysis, we first visualize and quantify the representations learned by our approach. Then we analyze the dynamics of the radius parameter during training. At last, we conduct representation analysis at the instance level.

A.1 Visualization.

We also use *t*-SNE (van der Maaten and Hinton, 2008) to visualize the embedding before and after training, by ProtoNet and HyperProto, respectively. 5 classes are sampled from the training set and test set of the Few-NERD dataset, and for each class, 500 samples are randomly chosen to be embedded by BERT trained on the 5-way-5-shot NER task. Figure 7 shows the result of embeddings in a 2-dimensional space, where different colors represent classes. Note that for the token-level NER task, the interaction between the target token and its context may result in a more mixed-up distribution compared to instance-level embedding. For both models, the representations of the same class in the training set become more compressed and easier to classify compared to their initial embeddings. While HyperProto can produce even more compact clusters. The clustering effect is also observed for novel classes. We also calculate the difference between the mean euclidean distances from each class sample to the (hypersphere) prototype of the target class and to other classes. The larger the difference, the better the samples are distinguished. For ProtoNet, the difference is 2.33 and 1.55 on the train and test set, while for HyperProto the results are 5.09 and 4.56, respectively. This can also be inferred from the *t*-sne result. Since samples from different classes are distributed at different densities, an extra radius parameter will help better distinguish between classes. The visualization and statistical results demonstrate the effectiveness of HyperProto in learning discriminative features, especially in learning novel class representation that considerably boosts model performance under few-shot settings.

A.2 Impact of Number of Shots

We conduct additional experiments on FEW-NERD (INTRA) 5-way setting with 10, 15, 20 shots. Since NNShot becomes too memory-intensive to run when shot reaches 15, we provide results on Proto and HyperProto. Figure 8

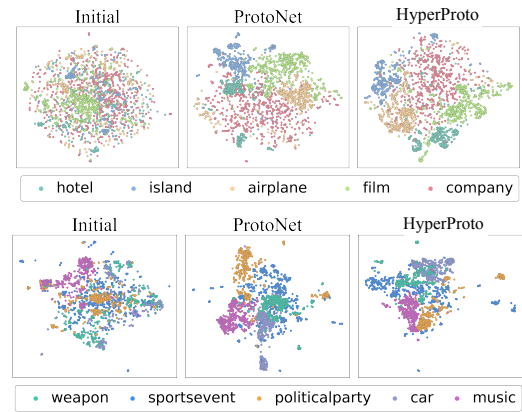


Figure 7: *t*-sne visualization of feature distributions. The six subfigures, from left to right, are the representations of seen data (in training set) before training, produced by ProtoNet, and produced by HyperProto; novel data (in test set) before training, produced by ProtoNet, and produced by HyperProto. Note that even after training, the neural network has never seen the novel data and their classes.

shows both models perform better when more data are available, while HyperProto performs consistently better than vanilla prototypes.

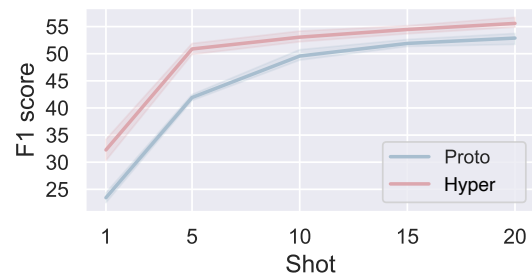


Figure 8: Impact of shot number on model performance for FEW-NERD (INTRA) 5-way setting.

B Experimental Details

This section reports the experimental details of all three tasks in our evaluation. All the experiments are conducted on NVIDIA A100 and V100 GPUs with CUDA. The main experiments are conducted on three representative tasks in NLP and CV, which are few-shot named entity recognition (NER), relation extraction (RE), and image classification. The experimental details will be presented in the following sections.

B.1 Experimental Details for Few-shot Named Entity Recognition

We assess the effectiveness of hypersphere prototypes on NLP, specifically, the first task is few-shot named entity recognition (NER) and the dataset is FEW-NERD (Ding et al., 2021c)². NER aims at locating and classifying named entities (real-world objects that can be denoted with proper names) given an input sentence, which is typically regarded as a sequence labeling task. Given an input sentence "Bill Gates is a co-founder of the American multinational technology corporation Microsoft", an named entity recognition system aims to locate the named entities (*Bill Gates*, *Microsoft*) and classify them into specific types. Conventional schema uses coarse-grained labels such that *Person* for *Bill Gates* and *Organization* for *Microsoft*. In more advanced schema like FEW-NERD, models are asked to give more specific entity types, for example, *Person-Entrepreneur* for *Bill Gates* and *Organization-Company* for *Microsoft*. Different from typical instance-level classification, few-shot NER is a sequence labeling task, where labels may share structural correlations. NER is the first step in automatic information extraction and the construction of large-scale knowledge graphs. Quickly detecting fine-grained unseen entity types is of significant importance in NLP. To capture the latent correlation, many recent efforts in this field use large pre-trained language models (Han et al., 2021) like BERT (Devlin et al., 2019) as backbone model and have achieved remarkable performance. The original prototypical network has also been applied to this task (Li et al., 2020b; Huang et al., 2020; de Lichy et al., 2021).

Dataset. The experiment is run on FEW-NERD dataset (Ding et al., 2021c). It is a large-scale NER dataset containing over 400,000 entity mentions, across 8 coarse-grained types and 66 fine-grained types, which makes it an ideal dataset for few-shot learning. It has been shown that existing methods including prototypes are not effective enough on this dataset.

Baselines. NNShot (Yang and Katiyar, 2020) is a token-level metric-based method that is specifically designed for few-shot labeling. Note that the main baseline here is the Proto method, which adapts the prototypical network on few-shot named entity recognition.

Implementation Details. We run experiments

under four settings on the two released benchmarks, FEW-NERD (INTRA) and FEW-NERD (INTER). Specifically, we use uncased BERT as the backbone encoder and $1e-4$ as the encoder learning rate. We manually tune the learning rate for the radius parameter, and the best result is obtained with 10. AdamW is used as the BERT optimizer, and Adam (Kingma and Ba, 2017) is used to optimize prototype radius. The batch size is set to 2 across all settings. All models are trained for 10000 steps and validated every 1000 steps. The results are reported on 5000 steps of the test episode. For each setting, we run the experiment with 3 different random seeds and report the average results including precision, recall, f1-score, and the standard error for each. We use PyTorch (Paszke et al., 2019) and huggingface transformers (Wolf et al., 2020) to implement the backbone encoder BERT_{base}.

B.2 Experimental Details for Few-shot Relation Extraction

The other common NLP task is relation extraction (RE), which aims at correctly classifying the relation between two given entities in a sentence. For example, given an input sentence with marked entities "[*Bill Gates*] is a co-founder of the American multinational technology corporation [*Microsoft*]", the relation extraction system aims to give the relationship between *Bill Gates* and *Microsoft*. This is a fundamental task in information extraction. RE is an important form of learning structured knowledge from unstructured text. We use FewRel (Han et al., 2018)³ and FewRel 2.0 (Gao et al., 2019b) as the datasets. In real-world datasets, many of the relations are long-tailed and thus cannot be identified accurately under the common supervised setting. Traditional methods often alleviate the problem with distant supervision, which would result in wrong labels. Recent approaches have applied few-shot learning models on the task to learn from a handful of samples, which yield promising results (Gao et al., 2019a). We report the datasets, baselines, and experimental details in Appendix B.2.

Dataset. We adopt the FewRel dataset (Han et al., 2018; Gao et al., 2019b), a relation extraction dataset specifically designed for few-shot learning. FewRel has 100 relations with 700 labeled instances each. The sentences are extracted from Wikipedia and the relational entities are obtained

²FEW-NERD is distributed under CC BY-SA 4.0 license

³FewRel is distributed under MIT license

from Wikidata. FewRel 1.0 (Han et al., 2018) is released as a standard few-shot learning benchmark. FewRel 2.0 (Gao et al., 2019b) adds domain adaptation task and NOTA task on top of FewRel 1.0 with the newly released test dataset on PubMed corpus.

Baselines. In addition to the main baseline, prototypical network (Snell et al., 2017), we also choose the following few-shot learning methods as the baselines in relation extraction. (1) Proto-HATT (Gao et al., 2019a) is a neural model with hybrid prototypical attention. (2) MLMAN (Ye and Ling, 2019) is a multi-level matching and aggregation network for few-shot relation classification. Note that Proto-HATT and MLMAN are not model-agnostic. (3) GNN (Satorras and Estrach, 2018) is a meta-learning model with a graph neural network as the prediction head. (4) SNAIL (Mishra et al., 2017) is a meta-learning model with attention mechanisms. (5) Meta Net (Munkhdalai and Yu, 2017) is a classical meta-learning model with meta information. (6) Proto-ADV (Gao et al., 2019b) is a prototype-based method enhanced by adversarial learning. (7) BERT-pair (Gao et al., 2019b) is a strong baseline that uses BERT for few-shot relation classification. We re-run all the baselines, except for MLMAN, and report the corresponding performances.

Implementation Details The experiments are conducted on FewRel 1.0 and FewRel 2.0 domain adaptation tasks. For FewRel 1.0, we follow the official splits in Han et al. (2018). For FewRel2.0, we follow Gao et al. (2019b), training the model on wiki data, validating on SemEval data, and testing on the PubMed data. We use the same CNN structure and BERT as encoders. The learning rate for hypersphere prototype radius is 0.1 and 0.01 for CNN and BERT encoder, respectively. Adam (Kingma and Ba, 2017) is used as radius optimizer. We train the model for 10000 steps, validate every 1000 steps, and test for 5000 steps. The other hyperparameters are the same as in the original paper.

B.3 Experimental Details for Few-shot Image Classification

Image classification is one of the most classical tasks in few-shot learning research. Seeking a better solution for few-shot image classification is beneficial in two ways: (1) to alleviate the need for data augmentation, which is a standard technique to enrich the labeled data by performing transformations on a given image; (2) to facilitate the applica-

tion where the labeled image is expensive. We use *miniImageNet* (Vinyals et al., 2016) as the dataset in our experiment. The dataset, baselines and experimental details are reported in Appendix B.3.

Dataset. *miniImageNet* (Vinyals et al., 2016) is used as a common benchmark for few-shot learning. The dataset is extracted from the full ImageNet dataset (Deng et al., 2009), and consists of 100 randomly chosen classes, with 600 instances each. Each image is of size $3 \times 84 \times 84$. We follow the split in (Ravi and Larochelle, 2017) and use 64, 16, and 20 classes for training, validation, and testing.

Baselines. The baselines we choose are as follows: (1) Prototypical network (Snell et al., 2017) is our main baseline; (2) IMP (Allen et al., 2019) is a prototype-enhanced method that models an infinite mixture of prototypes for few-shot learning; (3) CovaMNet (Li et al., 2019a) is a few-shot learning method that uses covariance to model the distribution information to enhance few-shot learning performance. (4) SNAIL (Mishra et al., 2017) is an attention-based classical meta-learning method; (5) Variational FSL (Zhang et al., 2019) is a variational Bayesian framework for few-shot learning, which contains a pre-training stage; (6) Activation to Parameter (Qiao et al., 2018) predicts parameters from activations in few-shot learning; (7) LEO (Rusu et al., 2018) optimizes latent embeddings for few-shot learning. (8) TRAML (Li et al., 2020a) uses adaptive margin loss to boost few-shot learning, and Prototypes + TRAML is a strong baseline in recent years.; (9) Meta-baseline (Chen et al., 2021) is a pre-training & tuning method that serves as a strong baseline in few-shot learning.

Implementation Details. The experiments are conducted on 5 way 1 shot and 5 way 5 shot settings. To ensure validity and fairness, we implement hypersphere prototypes with various backbone models including CNN, ResNet-12, and WideResNet (Zagoruyko and Komodakis, 2016) to make it comparable to all baseline results, and we also re-run some of the baselines including prototypical network (Snell et al., 2017), infinite mixture prototypes (Allen et al., 2019), and CovaMNet (Li et al., 2019a) under our settings based on their original code. Other baseline results are taken from the original paper. Each model is trained on 10,000 randomly sampled episodes for 30~40 epochs and tested on 1000 episodes. The result is reported with 95% confidence interval. Note that both ResNet-12 and WideResNet (Zagoruyko and

Komodakis, 2016) are pretrained on the training data, where the pretrained ResNet-12 is identical to Chen et al. (2021) and the pretrained WideResNet follows Mangla et al. (2020). The CNN structure is the same as Snell et al. (2017), which is composed of 4 convolutional blocks each with a 64-filter 3×3 convolution, a batch normalization layer (Ioffe and Szegedy, 2015), a ReLU nonlinearity, and a 2×2 max-pooling layer. We use SGD optimizer for the encoder and Adam (Kingma and Ba, 2017) optimizer for the prototype radius. The learning rate for the backbone model is $1e-3$. The learning rate for radius is manually tuned and the reported result in Table 3 has a learning rate of 10. For cone-like and gaussian prototypes, we use $1e-1$ and $1e-3$. At the training stage, the prototype center is re-initialized at each episode as the mean vector of the support embeddings.

C Discussion

This section discusses other related prototype-based methods in detail, as well as limitations and broader impact of our work.

C.1 Other Prototype-enhanced Methods

Here, we discuss the difference between hypersphere prototypes with four prototype-enhanced methods in few-shot learning: infinite mixture prototypes (Allen et al., 2019), CovaMNet (Li et al., 2019a), variational few-shot learning (Zhang et al., 2019), and two-stage (Das and Lee, 2020).

Infinite mixture prototypes (Allen et al., 2019) model each class as an indefinite number of clusters and the prediction is obtained by computing and comparing the distance to the nearest cluster in each class. This method is an intermediate model between prototypes and the nearest neighbor model, whereas hypersphere prototypes alleviate the over-generalization problem of vanilla prototypes with a single additional parameter that turns a single point modeling into a hypersphere. The essential prototype-based feature of hypersphere prototypes allows faster computation and easier training.

CovaMNet (Li et al., 2019a) calculates local variance for each class based on support samples and conducts metric-based learning via covariance metric, which basically evaluates the cosine similarity between query samples and the eigenvectors of the local covariance matrix. To ensure the non-singularity of the covariance matrix, the feature of each sample is represented with a matrix, generated

by a number of local descriptors, with each extracting a feature vector. Compared to hypersphere prototypes, both methods attempt to model more variance based on vanilla prototypes, while the idea of hypersphere prototypes is more straightforward and requires fewer parameters. On the other hand, the multi-channel features adopted by CovaMNet are less natural for NLP tasks.

Variational Few-Shot Learning (Zhang et al., 2019) tackles the few-shot learning problem under a bayesian framework. In order to improve single point-based estimation, a class-specific latent variable representing the class distribution is introduced and is assumed to be Gaussian. The method parameterizes the mean and variance of the latent variable distribution with neural networks that take the feature of a single instance as input. The learning and inference processes are both conducted on the latent variable level. The method adopts variational inference and is built on modeling distribution as a latent variable, where the metric calculation highly relies on the Gaussian assumption. Hypersphere prototypes, on the other hand, model the distribution with a center vector and a radius parameter in the actual embedding space, which is more tangible and easier to calculate. It is worth noting that this work also points that a single embedding is insufficient to represent a class, and samples the prototype from a high-dimensional distribution. This is actually similar to our starting point, the difference is that our approach turns out to consider the problem from the geometric point of view based on the original embedding space, and proves that such simple geometric modeling could be very efficient in the few-shot scenarios.

Two-Stage Approach first trains feature encoder and variance estimator on training data in an episodic manner with extracted absolute and relative features. Then in the second stage, training data are split into "novel" class, and base class, novel class prototypes are learned from both sample mean and base class features. The classification is carried out with integrated prototypes. This method improves on vanilla prototypes by extracting more features and combining information from base classes, but still follows single-point-based metric learning. Our approach extends a single point to a hypersphere in the embedding space and therefore, better captures within-class variance.

Algorithm 2: Greedy N -way $K \sim 2K$ -shot sampling algorithm for FEW-NERD

Input: Dataset \mathcal{X} , Label set \mathcal{Y} , N , K

Output: output result

$\mathcal{S} \leftarrow \emptyset$; // Init the support set

// Init the count of entity types

for $i = 1$ to N **do**

 Count[i] = 0 ;

repeat

 Randomly sample $(x, y) \in \mathcal{X}$;

 Compute |Count| and Count $_i$ after update ;

if |Count| > N or \exists Count[i] > $2K$ **then**

 Continue ;

else

$\mathcal{S} = \mathcal{S} \cup (x, y)$;

 Update Count $_i$;

until Count $_i \geq K$ for $i = 1$ to N ;

C.2 Limitations

Under the 1-shot setting, hypersphere prototypes will face challenges in estimating the radius in support sets, this is because the initial radius may be biased by the randomness of sampling. When the radius is set to exactly 0, the model will resemble a traditional prototypical network. In our empirical study, we find that setting radius could consistently yield more robust performance than traditional ways. Although not as large as the boost in the multi-shot setting, our method in the 1-shot scenario still delivers non-trivial results and exceeds most baselines (Table 1, Table 2, Table 3).

C.3 Broader Impact

Our method focuses on the method of few-shot learning, which enables machine learning systems to learn with few examples, and could be applied to many downstream applications. The technique itself does not have a direct negative impact, i.e., its impact stems primarily from the intent of the user, and there may be potential pitfalls when the method is applied to certain malicious applications.

D $K \sim 2K$ Sampling for Few-NERD

In the sequence labeling task FEW-NERD, the sampling strategy is slightly different from other classification tasks. Because in the named entity recognition, each token in a sequence is asked to be labeled as if it is a part of a named entity. And the context is crucial for the classification of each entity, thus the examples are sampled at the sequence

level. Under this circumstance, it is difficult to operate accurate N way N shot sampling. Ding et al. (2021c) propose a greedy algorithm to conduct N way $K \sim 2K$ shot sampling for the FEW-NERD dataset. We follow the strategy of the original paper (Ding et al., 2021c) and report it in Algorithm 2.